Available online at www.sciencedirect.com
ScienceDirect
Analytical Biochemistry 364 (2007) 128–137
ANALYTICAL BIOCHEMISTRY
www.elsevier.com/locate/yabio

Analysis of mitochondrial subunit assembly into respiratory chain complexes using Blue Native polyacrylamide gel electrophoresis

Matthew McKenzie [a,*], Michael Lazarou [a], David R. Thorburn [b,c], Michael T. Ryan [a,*]

[a] *Department of Biochemistry, La Trobe University, Melbourne, VIC 3086, Australia*
[b] *Murdoch Children's Research Institute and Genetic Health Services Victoria, Royal Children's Hospital, University of Melbourne, Melbourne, VIC 3052, Australia*
[c] *Department of Pediatrics, University of Melbourne, Melbourne, VIC 3052, Australia*

Received 23 November 2006
Available online 24 February 2007

Abstract

The mitochondrial respiratory chain consists of multi-subunit protein complexes embedded in the inner membrane. Although the majority of subunits are encoded by nuclear genes and are imported into mitochondria, 13 subunits in humans are encoded by mitochondrial DNA. The coordinated assembly of subunits encoded from two genomes is a poorly understood process, with assembly pathway defects being a major determinant in mitochondrial disease. In this study, we monitored the assembly of human respiratory complexes using radiolabeled, mitochondrially encoded subunits in conjunction with Blue Native polyacrylamide gel electrophoresis. The efficiency of assembly was found to differ markedly between complexes, and intermediate complexes containing newly synthesized mitochondrial DNA-encoded subunits could be observed for complexes I, III, and IV. In particular, we detected human cytochrome *b* as a monomer and as a component of a novel approximately 120 kDa intermediate complex at early chase times before being totally assembled into mature complex III. Furthermore, we show that this approach is highly suited for the rapid detection of respiratory complex assembly defects in fibroblasts from patients with mitochondrial disease and, thus, has potential diagnostic applications.
© 2007 Elsevier Inc. All rights reserved.

Keywords: Mitochondria; Supercomplex; Membrane protein; Blue native PAGE; OXPHOS

Mitochondria provide the main energy source for eukaryotic cells, oxidizing sugars and fats to generate ATP via oxidative phosphorylation (OXPHOS)[1]. This is accomplished by the respiratory chain, a series of multimeric enzyme complexes of the inner mitochondrial membrane comprising complex I (NADH-ubiquinone oxidoreductase, EC 1.6.5.3), complex II (succinate-ubiquinone oxidoreductase, EC 1.3.5.1), complex III (ubiquinol-ferricytochrome *c* oxidoreductase, EC 1.10.2.2), complex IV (cytochrome *c* oxidoreductase, EC 1.9.3.1), and complex V (F_1F_0 ATPase).

Defects in the respiratory chain result in human mitochondrial disease that leads to a wide variety and combination of clinical symptoms but regularly involves neurological and muscular disease (encephalomyopathy). Onset can be at any age, although severe childhood disease is common [1]. Although biochemical studies can assign mitochondrial enzymatic deficiencies in many cases, the pathophysiology still remains unclear. One complicating factor is the dual genetic control, with mitochondria containing their own circular, double-stranded genome. In humans, mitochondrial DNA (mtDNA) encodes 13

* Corresponding authors. Fax: +61 3 9479 2467.
E-mail addresses: m.mckenzie@latrobe.edu.au (M. McKenzie), m.ryan@latrobe.edu.au (M.T. Ryan).

[1] *Abbreviations used:* OXPHOS, oxidative phosphorylation; mtDNA, mitochondrial DNA; tRNA, transfer RNA; rRNA, ribosomal RNA; BN–PAGE, Blue Native polyacrylamide gel electrophoresis; LIMD, lethal infantile mitochondrial disease; COX, cytochrome *c* oxidase; DMEM, Dulbecco's modified Eagle's medium; FBS, fetal bovine serum; CAP, chloramphenicol; CHX, cycloheximide; DDM, *n*-dodecyl-β-D-maltoside; BSA, bovine serum albumin; PVDF, polyvinylidene fluoride; HRP, horseradish peroxidase; ECL, electrochemiluminescence; 2D–PAGE, two-dimensional PAGE.

0003-2697/$ - see front matter © 2007 Elsevier Inc. All rights reserved.
doi:10.1016/j.ab.2007.02.022

polypeptides of the respiratory chain (7 for complex I, 1 for complex III, 3 for complex IV, and 2 for complex V) as well as 22 transfer RNAs (tRNAs) and 2 ribosomal RNAs (rRNAs) specific for mitochondrial translation. mtDNA-encoded subunits must assemble with nuclear-encoded subunits that are synthesized in the cytosol and imported into the organelle [2].

One method for the analysis of these mtDNA-encoded translation products is to selectively radiolabel them in vivo with [^{35}S]methionine. This technique has proved to be highly effective in the initial identification of some mtDNA protein-encoding genes [3,4] and has also been used to examine the effects of mtDNA disease-causing mutations on mitochondrial protein synthesis [5–8].

Another technique, Blue Native polyacrylamide gel electrophoresis (BN–PAGE), followed by immunodecoration, has proved to be invaluable for the analysis of individual respiratory complexes [9]. For example, complex I subcomplexes were identified in patients with complex I enzyme deficiencies and in normal cells after inhibiting mitochondrial protein synthesis [10–12]. This information, in conjunction with structural analysis, has been used to develop a number of models for complex I assembly [11,12]. BN–PAGE has also been used to examine the assembly of complex IV, identifying two assembly intermediates that contain mtDNA-encoded subunits [13]. Individual respiratory complexes also exist in larger supercomplexes (or "respirasomes"), with the largest form (observed at ~1700 kDa on BN–PAGE) estimated to contain four copies of complex IV, two copies of complex III, and one copy of complex I [14]. This supercomplex is detergent labile and can dissociate into smaller supercomplexes as well as into holocomplexes [15,16]. Two recent studies identified that complex I stability is reliant on an intact complex III [17,18], and this may relate to the association of these complexes within a supercomplex. In addition, destabilized supercomplexes resulting from cardiolipin remodeling defects were detected by BN–PAGE in patients with Barth syndrome, highlighting the importance of supercomplex stability for respiratory chain function [19].

In this study, we combined radiolabeling and BN–PAGE analysis to monitor the synthesis and turnover of mtDNA-encoded subunits and their mode of assembly into complexes I, III, IV, and V. Using this approach, assembly intermediates were detectable at early chase times for complexes I and IV, with a novel intermediate described for human complex III. We also identified that complex assembly defects can be observed directly in cells from patients diagnosed with mitochondrial disease, highlighting the potential diagnostic use of this approach.

Materials and methods

Cell lines and culture conditions

143BTK$^-$ ρ^+ (wild-type) and 143B-87 ρ^0 (lacking mtDNA) osteosarcoma cells were a gift from I. Trounce (University of Melbourne). Fibroblast cell lines were derived from skin biopsies of control (wild-type) or mitochondrial disease patients with lethal infantile mitochondrial disease (LIMD) (patient A), cardiomyopathy (patient B), LIMD (*NDUFS6* deletion, patient C [15]), Leigh disease/cytochrome *c* oxidase (COX) deficiency (patient D), COX deficiency (*SURF1* mutation, patient E), or mitochondrial encephalomyopathy (patient F). Fibroblast enzyme activities were measured as described previously [20].

Cells were grown at 37 °C and 5% CO_2 in Dulbecco's modified Eagle's medium (DMEM, Invitrogen) supplemented with 10% (v/v) fetal bovine serum (FBS, Invitrogen), 50 μg/ml uridine, and 1 mM pyruvate.

Isolation of mitochondria from cultured cells was performed as described previously [19].

Labeling of mitochondrial encoded proteins

Mitochondrial translation products were specifically labeled using previously employed methods [21]. Approximately 2×10^5 cells were pretreated with 50 μg/ml chloramphenicol (CAP, Sigma) in DMEM containing 10% (v/v) FBS for 24 h before labeling. Cells subsequently were incubated with 0.1 mg/ml cycloheximide (CHX, Sigma) in 1 ml methionine-free DMEM containing 5% (v/v) dialyzed FBS for 15 min at 37 °C. Labeling was performed by the addition of 20 μCi of [^{35}S]methionine/cysteine (EXPRE^{35}S^{35}S Protein Labeling Mix, PerkinElmer Life Sciences) for 2 h, followed by the addition of cold methionine to a final concentration of 1 mM. After 15 min, the solution was removed and replaced with DMEM/10% (v/v) FBS for extended chase times.

SDS–PAGE

Tris–tricine SDS–PAGE was performed according to the method of Schagger and von Jagow [22]. Cell pellets (100 μg total protein) were prepared for electrophoresis by suspension in 50 mM Tris–Cl (pH 6.8), 2% (w/v) SDS, 100 mM dithiothreitol, and 10% (v/v) glycerol before separation on a 10 to 16% polyacrylamide Tris–tricine gradient gel at 100 V/25 mA for 14 h.

BN–PAGE

BN–PAGE was performed based on the method of Schagger and von Jagow [9] with minor modifications. Cell pellets (100 μg protein) were solubilized for 30 min on ice in 50 μl of 20 mM bis-Tris (pH 7.4), 50 mM NaCl, and 10% (v/v) glycerol containing either 1% (w/v) digitonin (Merck), 1% (w/v) Triton X-100 (Sigma), or 0.2% (w/v) *n*-dodecyl-β-D-maltoside (DDM, Sigma). Insoluble material was removed by centrifugation at 18,000 *g* for 5 min at 4 °C, with the soluble component combined with BN–PAGE loading dye (final concentrations: 0.5% [w/v] Coomassie Blue G, 50 mM ε-amino *n*-caproic acid [Sigma],

10 mM bis-Tris [pH 7.0]), and separated on a 4 to 13% acrylamide–bisacrylamide BN–PAGE gel (in 70 mM ε-amino *n*-caproic acid and 50 mM bis-Tris [pH 7.0]) using an SE600 Electrophoresis Unit (Hoefer). For separation, cathode buffer (15 mM bis-Tris [pH 7.0] and 50 mM tricine) containing 0.02% (w/v) Coomassie Blue G was used until the dye front had reached approximately one-third of the way through the gel before exchange with cathode buffer lacking Coomassie Blue G. Anode buffer contained 50 mM bis-Tris (pH 7.0). Native complexes were separated at 100 V/5 mA for 13.5 h at 4 °C. Thyroglobulin (669 kDa), ferritin (440 kDa), and bovine serum albumin (BSA, 140 and 67 kDa) were used as markers.

Two-dimensional PAGE

BN–PAGE strips were sandwiched between two glass plates before pouring of a 10 to 16% polyacrylamide Tris–tricine gradient gel and stacking gel [22]. Samples were separated in the second dimension at 100 V/25 mA for 14 h.

Western transfer

Following electrophoresis, gels were soaked in 48 mM Tris–Cl, 39 mM glycine, 0.0037% (w/v) SDS, and 20% (v/v) methanol for 20 min before transfer to polyvinylidene fluoride (PVDF) membrane (Immobilon, Millipore) at 400 mA for 1.5 h. Membranes were stained with 0.1% (w/v) Coomassie Blue R/50% (v/v) methanol/7% (v/v) acetic acid, destained with 50% (v/v) methanol/7% (v/v) acetic acid, further destained with 90% (v/v) methanol/10% (v/v) acetic acid, and then air-dried.

Protein detection

Dried membranes were developed with phosphor intensifying screens using a Typhoon phosphorimager (Molecular Diagnostics). After this, membranes were rewetted briefly with 100% methanol and then blocked with 10% (w/v) skim milk powder in 1× phosphate-buffered saline (PBS, 137 mM NaCl, 2.7 mM KCl, 10 mM Na_2HPO_4, and 2 mM KH_2PO_4) containing 0.05% (v/v) Tween 20 for 2 h. Membranes were washed before incubating with primary antibodies overnight at 4 °C. Mouse monoclonal antibodies (Invitrogen) used included the anti-70 kDa (complex II), anti-core I (complex III), anti-subunit I (complex IV), and anti-alpha subunit (complex V). The anti-ND1 antibody was a gift from A. Lombes (INSERM). A rabbit polyclonal antibody to the human complex I 39 kDa subunit (NDUFA9) was raised against recombinant, bacterially expressed protein as described previously [23]. Secondary probing with anti-mouse or anti-rabbit horseradish peroxidase (HRP)-conjugated antibodies (Sigma) was performed for 2 h, followed by detection using electrochemiluminescence (ECL) reagents (Amersham) and a Chemi-Genius Bioimaging System (Syngene).

Results

Mitochondrial translation product labeling and complex formation

Newly synthesized mtDNA-encoded subunits can be specifically labeled by incubating cells with [^{35}S]methionine/cysteine in the presence of CHX, which blocks cytosolic protein synthesis [21]. To stabilize these subunits, nuclear-encoded subunits were first accumulated in mitochondria by pretreating cells with CAP [24]. Assembly of mtDNA-encoded subunits into respiratory complexes was monitored by the further incubation of cells following the removal of radiolabel and translation inhibitors (Fig. 1A, "chase"). 143BTK$^-$ ρ^+ (wild-type) osteosarcoma cells were harvested and proteins were separated on SDS–PAGE followed by phosphorimage analysis (Fig. 1B, lanes 1–4). MtDNA-encoded translation products were specifically labeled when cells were incubated with CHX (Fig. 1B, lane 2), and their identities were assigned according to previously published profiles [21]. In the absence of CHX, a multitude of proteins, including nuclear-encoded translation products, were labeled (Fig. 1B, lane 4). CAP pretreatment appeared to increase the specificity and stability of

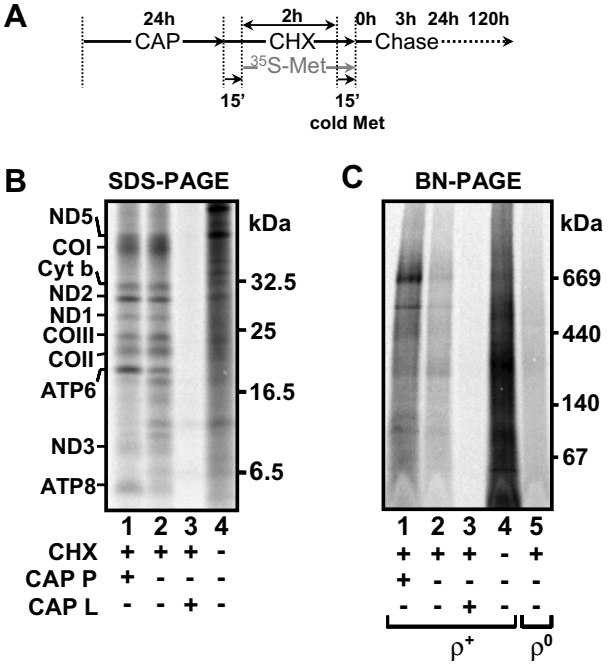

Fig. 1. mtDNA subunit translation and assembly. (A) Schematic depicting labeling procedure. Cells were incubated with CAP for 24 h, followed by a 15-min CHX incubation before pulse labeling with [^{35}S]methionine/cysteine for 2 h. After a 15-min chase with 0.1 mM cold methionine, cells were harvested (0 h) or chased for longer periods. (B,C) Wild-type (ρ^+) and mtDNA-less (ρ^0) 143BTK$^-$ osteosarcoma cells were labeled with [^{35}S]methionine/cysteine in the absence (lane 4) or presence (lanes 1–3 and 5) of CHX. CAP pretreatment (CAP P, lane 1) and labeling in the presence of CAP (CAP L, lane 3) were also performed. Cells were analyzed by SDS–PAGE (B) or were solubilized in 0.2% (w/v) DDM (1 g/g protein) and separated by BN–PAGE (C) before phosphorimage analysis.

mitochondrial translation products, and this is particularly evident with the ATP8 subunit (Fig. 1B, cf. lanes 1 and 2). As expected, incubation of cells with both CHX and CAP prevented any protein labeling (Fig. 1B, lane 3).

To determine whether newly synthesized mtDNA-encoded translation products efficiently assembled into respiratory complexes, total cell pellets were solubilized in DDM and subjected to BN–PAGE followed by phosphorimage analysis (Fig. 1C). This detergent has been well used for the solubilization of respiratory chain complexes and analysis by BN–PAGE [11,14,25]. Complexes of approximately 650 and 500 kDa were observed in cells treated with CHX (Fig. 1C, lanes 1 and 2) and even more readily in cells pretreated with CAP (Fig. 1C, lane 1). These complexes were not clearly observed in cells containing both labeled cytosolic and mitochondrial translation products (Fig. 1C, lane 4) or when CAP was retained during the labeling with CHX (Fig. 1C, lane 3). The complexes were also absent in 143B ρ^0 cells that lack mtDNA (Fig. 1C, lane 5), indicating that they are respiratory complexes and/or their assembly intermediates.

Assembly of mtDNA-encoded subunits into respiratory complexes

Although four of the respiratory chain complexes contain mtDNA-encoded subunits, only two complexes (migrating at ~650 and 500 kDa) were clearly observed after 2 h labeling. Other less intense complexes were also visible in the lower molecular weight range (Fig. 1C, lane 1). The approximately 650 kDa complex might represent assembly of new subunits into complex V and/or into the complex III_2/IV supercomplex. Other newly translated subunits may require longer maturation times before they can fully assemble into their respective complexes. To test this, we incubated cells with [^{35}S]methionine/cysteine in the presence of CHX to label mtDNA-encoded subunits and then incubated with cold methionine before harvesting at different chase time points. Each total cell sample was then split in three and solubilized in buffer containing digitonin, DDM, or Triton X-100 detergents before BN–PAGE analysis (Fig. 2). Digitonin is known to retain complexes in their supercomplex forms, whereas high amounts of Triton X-100 completely dissociate the supercomplexes [16]. DDM has been shown previously to completely disrupt supercomplexes [14], although in our hands only partial disruption was observed [15,19].

In addition to the approximately 650 and 500 kDa complexes detected in Fig. 1C, other high-molecular weight complexes appeared after a chase period (Fig. 2A). In digitonin-solubilized cells, an approximately 1.7-MDa supercomplex (CI/$CIII_2$/CIV, formed by complexes I, III, and IV) is visible from 24 to 72 h chase, stabilizing in intensity after 48 h chase (Fig. 2, lanes 3–5). A faster migrating, approximately 1.5-MDa supercomplex is also faintly visible in the digitonin samples but is much greater in intensity in the DDM-solubilized samples (Fig. 2, lanes 7–10), consistent with a supercomplex containing complex I and III but lacking complex IV (CI/$CIII_2$). This loss of complex IV from the supercomplex is associated with the appearance of monomeric complex IV (CIV) during the chase (Fig. 2A, lanes 7–10). Some monomeric complex I (CI) can also be seen after extended chase periods in the DDM-solubilized extracts; however, most is found in the supercomplex (Fig. 2, lanes 6–10). In Triton X-100 extracts, no supercomplexes are visible and all individually labeled respiratory complexes can be seen during the chase period: complex I (CI) at approximately 980 kDa, complex V (CV) at approximately 650 kDa, complex III dimer ($CIII_2$) at approximately 500 kDa, and complex IV (CIV) at approximately 200 kDa (Fig. 2A, lanes 13–15).

In addition to the mature respiratory complexes, a number of other labeled complexes can be seen. In particular, a complex at approximately 800 kDa is present at early chase times in digitonin and Triton X-100 (Fig. 2A, CI_i, lanes 1, 2, 11, and 12). This complex most likely represents an assembly intermediate of complex I due to the fact that complex I (in Triton X-100 extracts) or the complex I/III_2/IV supercomplex (in digitonin extracts) appears following its disappearance. Furthermore, the CI_i complex is identical in size to the recently reported late complex I assembly intermediate that contains the assembly factor B17.2L [26] (data not shown).

To confirm the identities of the steady-state complexes, Western blots were also performed (Fig. 2B). As can be seen, digitonin solubilization retains the respiratory complexes in their supercomplex forms (Fig. 2B, lanes 1–3), with some complex III also seen in its dimeric form (minor amounts of complex IV are also visible). In DDM, the supercomplexes partially dissociate, leading to the detection of some monomeric complex I and complex IV (Fig. 2B, lanes 5–7), whereas in Triton X-100, no supercomplexes are observed (Fig. 2B, lanes 9–12). Note that complex V is not part of the supercomplexes and that the complex III dimer ($CIII_2$) and monomeric complex IV (CIV) migrate slower on BN–PAGE after digitonin solubilization compared with either DDM or Triton X-100.

Analysis of respiratory complex assembly intermediates

To confirm the subunit makeup of radiolabeled complexes and the presence of potential assembly intermediates, two-dimensional PAGE (2D–PAGE) was performed. Following labeling (0 h) or after 120 h chase, wild-type human fibroblasts were solubilized in 0.2% (w/v) DDM and subjected to BN–PAGE in the first dimension and to SDS–PAGE in the second dimension (Fig. 3A). Strongly labeled ATP8 and ATP6 subunits migrated at approximately 650 kDa, in agreement with the most prominently labeled species on BN–PAGE representing assembled complex V (Fig. 3A, CV, left panel). These two subunits were detected in abundance at both 0 and 120 h chase in the mature complex, suggesting that assembly of these subunits into the holoenzyme occurs rapidly. For

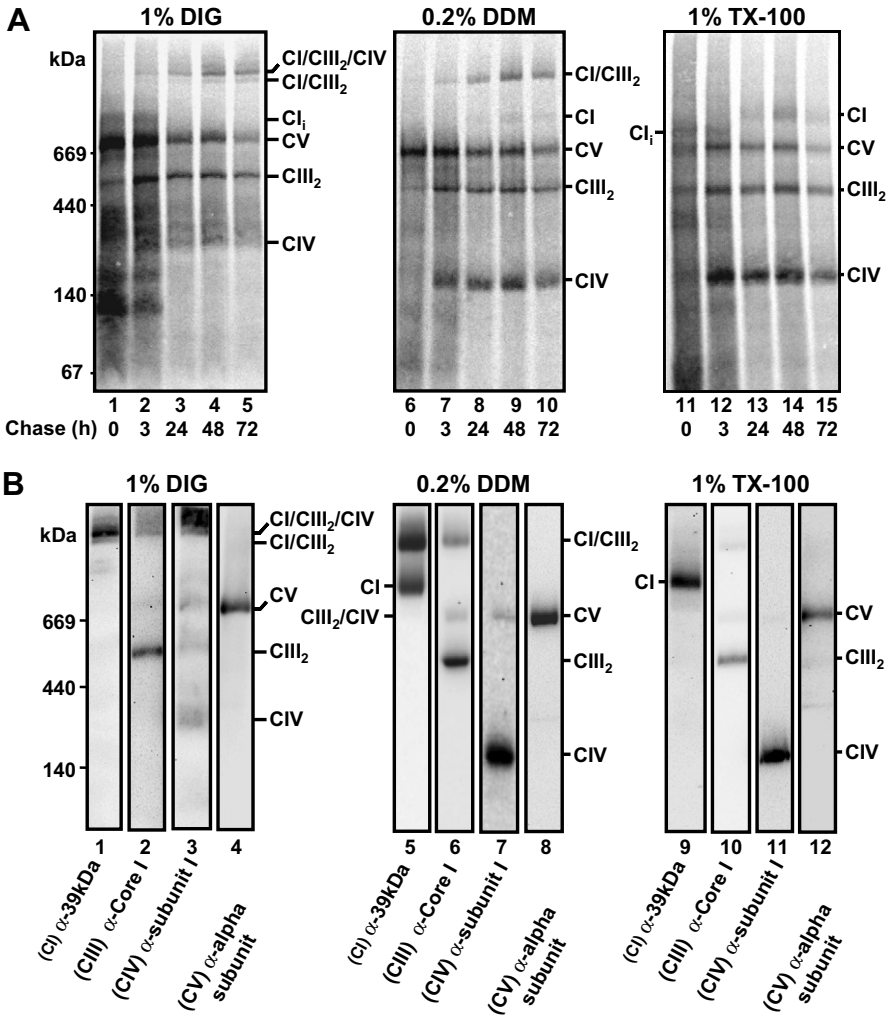

Fig. 2. Efficient assembly into holoenzymes and supercomplexes requires chase periods. Following pulse labeling, wild-type 143BTK$^-$ cells (100 μg total protein) were solubilized in either 1% (w/v) digitonin (DIG, 5 g/g protein, lanes 1–5), 0.2% (w/v) DDM (1 g/g protein, lanes 6–10), or 1% (w/v) Triton X-100 (TX-100, 5 g/g protein, lanes 11–15) and were separated by BN–PAGE. The gel subsequently was transferred to PVDF for phosphorimage analysis (A) or immunodecoration with antibodies to mitochondrial respiratory chain subunits (B). CI/CIII$_2$/CIV, complex I/III/IV supercomplex; CI/CIII$_2$, complex I/III supercomplex; CI, monomeric complex I; CV, complex V; CIII$_2$, complex III homodimer; CIV, monomeric complex IV; CI$_i$, complex I assembly intermediate.

complex I (CI), ND4, ND2, and ND1 were assigned according to their molecular weights and their presence in mature complex I (CI, ~980 kDa) as well as the complex I/III$_2$ supercomplex (~1.5 MDa) following 120 h chase (Fig. 3A, middle panel). ND1 was also identified by Western blot with its respective antibody (Fig. 3A, right panel). Two additional subunits at the low-molecular weight range were weakly labeled and most likely represent ND6 (~16.7 kDa) and ND3 (~13.5 kDa). ND4L (~14.8 kDa) and ND5 (~43.5 kDa) were not identified. At 0 h chase, ND subunits were found as monomers or in intermediate complexes (Fig. 3A, left panel), but by 120 h chase. they had assembled into complex I (CI) and the supercomplex (CI/CIII$_2$) (Fig. 3A, middle panel). For example, ND4 was found in an approximately 350 kDa intermediate complex at 0 h chase, and it was assembled into complex I (CI) and the supercomplex (CI/CIII$_2$) at 120 h chase.

Other respiratory complex assembly intermediates have been identified previously, particularly for complex IV [13,27]. Indeed, complex IV subunit 1 (CO1) was found in a low-molecular weight species of approximately 100 kDa (Fig. 3A, CIV$_i$, left panel). This may correspond to the previously identified S2 subcomplex of complex IV [13]. By 120 h, complex IV subunit 1 was fully chased from this approximately 100 kDa species to the mature sized complex at approximately 200 kDa (Fig. 3A, CIV, middle panel). Complex IV subunits 2 and 3 (CO2 and CO3) migrate together on SDS–PAGE, and at least one of these was also found in the approximately 100 kDa species CIV$_i$ prior to the chase (Fig. 3A, left panel). Some label was also seen in the monomeric range (~23 kDa) as well as within mature complex IV (CIV, ~200 kDa) at 0 h chase. Following the chase at 120 h, all labeled complex IV subunits 2 and 3 appeared in the mature complex IV holoenzyme

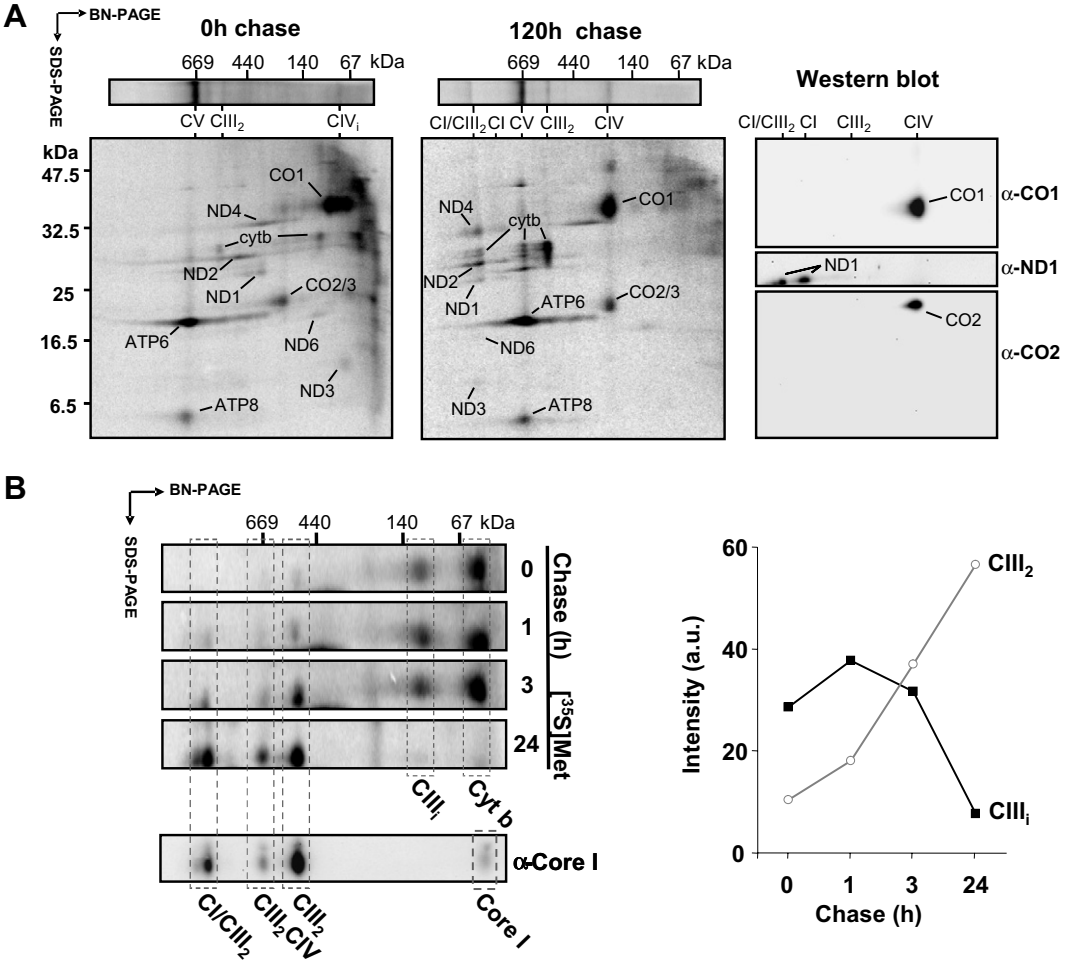

Fig. 3. Detection of mtDNA-encoded subunits in assembly intermediates. (A) [^{35}S]methionine/cysteine wild-type fibroblasts, after either a 0 or 120 h chase, were solubilized in DDM (1 g/g protein) and separated by 2D–PAGE (BN–PAGE in the first dimension and SDS–PAGE in the second dimension) followed by phosphorimage analysis. Positions of the radiolabeled mtDNA-encoded subunits are indicated. A BN–PAGE gel strip identical to that used in the 2D–PAGE is also shown. The identities of CO1, CO2, and ND1 were confirmed by Western blot (right panel). CI/CIII$_2$, complex I/III supercomplex; CI, monomeric complex I; CV, complex V; CIII$_2$, complex III homodimer; CIV, monomeric complex IV; CIV$_i$, complex IV assembly intermediate. (B) Following mtDNA-encoded protein labeling in 143BTK$^-$ cells, 130 μg of isolated mitochondria was solubilized in 1% (w/v) Triton X-100 (3.8 g/g protein) and analyzed by 2D–PAGE after various chase times. Radiolabeled cytochrome *b* was detected as a monomer (~30 kDa) in an approximately 120 kDa species (CIII$_i$), in the complex III dimer (CIII$_2$), and in the complex III$_2$/IV and CI/CIII$_2$ supercomplexes. The mobility of complex III in its dimeric and supercomplex forms was confirmed by immunodecoration with an antibody to the core I subunit of complex III (bottom left). Radiolabeled signal intensities of the approximately 120 kDa species (CIII$_i$) and the complex III dimer (CIII$_2$) during the chase period are shown at the right.

(CIV). Both complex IV subunits 1 and 2 were also detected at approximately 200 kDa in mature complex IV with their respective antibodies on Western blot (Fig. 3A, right panel).

The assembly of subunits into human complex III is not well understood, with most studies coming from yeast as a model [28–30]. At 0 h chase, the complex III subunit cytochrome *b* (running as a doublet) migrated at approximately 30 kDa (possible monomeric form) as well as in an approximately 120 kDa species (Fig. 3A, left panel) Some cytochrome *b* was also found at the position of the complex III dimer (Fig. 3A, CIII$_2$, ~500 kDa). Following the 120 h chase period, the subunit was found at positions corresponding to the complex III dimer (CIII$_2$, ~500 kDa), the complex III$_2$/IV supercomplex (CIII$_2$/CIV, ~700 kDa), and the complex I/III$_2$ supercomplex (CI/CIII$_2$, ~1.5 MDa) (Fig. 3A, middle panel).

To examine complex III assembly further, isolated mitochondria harboring labeled mtDNA-encoded translation products at various chase times were solubilized in 1% (w/v) Triton X-100 and analyzed by 2D–PAGE using a 10 to 16% Tris–tricine gradient gel for the second dimension (Fig. 3B, left panels). In this instance, the detergent to mitochondrial protein ratio was lowered from 5.0:1 g to 3.8:1 g, resulting in some detectable CI/CIII$_2$ and CIII$_2$/CIV supercomplexes. Again, what appears to be monomeric cytochrome *b* is detected at approximately 30 kDa up to 3 h chase and by 24 h chase is completely assembled into higher molecular weight complexes. The approximately 120 kDa species (CIII$_i$) detected in

Fig. 3A is also present at 0 h chase, increasing in intensity up to 3 h chase before assembling into the complex III homodimer ($CIII_2$), the III_2/IV supercomplex ($CIII_2$/CIV), and the CI/$CIII_2$ supercomplex (Fig. 3B). Intensities of the radiolabeled cytochrome *b* signals in Fig. 3B show an increase in complex III dimer ($CIII_2$) between 3 and 24 h chase, corresponding with a decrease in $CIII_i$ species levels over the same time period (Fig. 3B, right panel).

Western blot analysis was also performed after 2D–PAGE to detect the positions of the $CIII_2$ dimer and the CI/$CIII_2$ and $CIII_2$/CIV supercomplexes using an antibody to the nuclear-encoded complex III subunit core 1 (Fig. 3B, α-core I, left panel). Radiolabeled cytochrome *b* was found to migrate at the same size of these complexes. The smaller approximately 120 and 30 kDa species were not detected by the anti-core I antibody, possibly due to the low steady-state levels of these species or the absence of the core I subunit in these complexes.

Respiratory complex assembly in patient cells

The characterization of respiratory complex assembly described above required relatively small numbers of cells (100 μg total protein/lane) and little downstream processing due to the use of total cell homogenates for BN–PAGE. Therefore, the methodology is amenable to the analysis of patient cells for diagnostic purposes. To test this, we analyzed the assembly of respiratory chain complexes in fibroblasts from patients diagnosed with mitochondrial disease. Cells were subjected to mtDNA-subunit labeling and then harvested at 0 h or after 48 h chase before solubilization in 0.2% DDM (w/v) and BN–PAGE analysis (Fig. 4A). Patients with complex I enzymatic deficiencies (but unknown genotype) presenting with LIMD (patient A) or cardiomyopathy (patient B) exhibited a total lack of complex I assembly, as indicated by a lack of labeled CI/$CIII_2$ supercomplex (Fig. 4A). A different LIMD patient (patient C) with a complex I enzymatic defect and a known deletion mutation in the *NDUFS6* gene [15] exhibited a smaller CI/$CIII_2$ supercomplex (Fig. 4A, asterisk [*]) with some full-size supercomplex remaining, consistent with earlier immunoblot analyses [15]. A patient with Leigh disease/COX deficiency (with unknown genotype) exhibited barely detectable complex IV (CIV) (Fig. 4A, patient D), whereas a second COX-deficient patient (*SURF1* mutation) had no detectable complex IV holoenzyme (Fig. 4A, patient E). Finally, a patient with a complex III enzymatic deficiency presenting with mitochondrial encephalomyopathy (also unknown genotype) had no assembled complex III ($CIII_2$) and virtually no CI/$CIII_2$ supercomplex (Fig. 4A, patient F). Complex III has previously been shown to be required for complex I assembly [17,18], and consistent with this, the levels of both complexes and the CI/$CIII_2$ supercomplex are affected in this patient.

Further analysis of cells from patients D and E using pulse/chase labeling revealed different defects in complex IV assembly (Fig. 4B). In patient D, the approximately

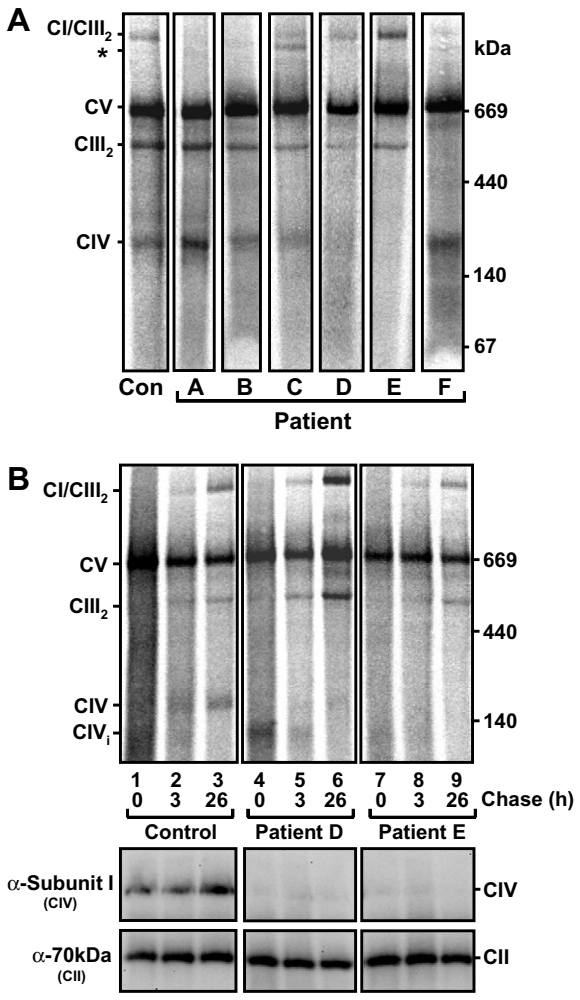

Fig. 4. Analysis of mtDNA-encoded subunit assembly in patient fibroblasts. (A) MtDNA-encoded subunits were radiolabeled in fibroblasts and subjected to a 48 h chase period. Cells (100 μg total protein) were solubilized in DDM, separated by BN–PAGE, and analyzed by phosphorimaging. Con, wild-type control; A, patient with LIMD (11% CI); B, patient with cardiomyopathy (35% CI); C, patient with LIMD (7% CI, *NDUFS6* deletion); D, patient with Leigh disease (27% CIV); E, patient with Leigh disease (14% CIV, *SURF1* mutation); F, patient with mitochondrial encephalomyopathy (6% CIII, 25% CI). Fibroblast residual enzyme activities are expressed as percentages of the control value relative to the mitochondrial marker enzyme citrate synthase; other respiratory chain enzyme activities were normal if not stated otherwise. CI/$CIII_2$, complex I/III supercomplex; CV, complex V; $CIII_2$, complex III homodimer; CIV, monomeric complex IV; CIV_i, complex IV assembly intermediate; *, intermediate CI/$CIII_2$ supercomplex. (B) Control, patient D (Leigh disease), and patient E (Leigh disease, *SURF1* mutation) fibroblasts after pulse/chase labeling. In patient D, the complex IV holoenzyme (CIV) is weakly detected with the intermediate (CIV_i) degraded over 26 h. In patient E, both CIV and CIV_i are undetectable. Immunoblots of complex IV and complex II steady-state levels are also shown (bottom panels).

100 kDa subcomplex (as described above as the possible S2 subcomplex [13]) was readily observed at 0 h (Fig. 4B, CIV_i, lane 4), but rather than being assembled into the holoenzyme, it was lost after 26 h chase (Fig. 4B, lane 6). In contrast, this intermediate subcomplex is absent in patient E, suggesting a defect at an earlier assembly stage

(Fig. 4B, lane 9). The *SURF1* mutation harbored by patient E is consistent with this model because the Surf1 protein is known to be involved in the early stages of complex IV assembly [31]. Both patients D and E have similarly depleted steady-state levels of mature complex IV as seen by Western blot analysis (Fig. 4B, lower panels); however, the pulse/chase analyses performed here revealed that they are the result of defects at different stages of the assembly pathway.

Discussion

In humans, the respiratory complexes of the mitochondrial inner membrane contain approximately 90 different subunits, with 13 encoded by mtDNA. Assembly of these complexes requires subunit expression from both mitochondrial and nuclear genomes as well as the involvement of various assembly factors, chaperones, and protein translocation components required for targeting and folding of subunits at the inner membrane. The complicated nature of this assembly has limited the generation of detailed models of the processes involved; thus, techniques are required for further study of respiratory complex biogenesis. Here we have combined the analysis of radiolabeled mtDNA-encoded subunits with BN–PAGE and have used this methodology in two ways: first, by performing pulse/chase studies to examine respiratory complex assembly and identify assembly intermediates and, second, by screening mitochondrial disease patient cell lines to identify missing or decreased levels of mature complexes and/or potential assembly pathway defects.

The overall labeling profile of mtDNA-encoded subunit assembly into respiratory complexes in human cells is surprising given the variable number of subunits incorporated into each complex. In particular, the levels of assembled complex I appear to be quite low in comparison with complex V. Complex I contains seven mtDNA-encoded subunits containing a total of 122 methionines, whereas complex V contains only two mtDNA-encoded subunits containing a total of 18 methionines. If there were an equal transcription and assembly rate of subunits as well as equal stoichiometries within complexes, the relative signal of radiolabeled complexes I/V should be approximately 7:1. However, it has been estimated that for bovine mitochondria, respiratory complexes are present in varying stoichiometries with a ratio of $1.1 \pm 0.2{:}1.3 \pm 0.1{:}3{:}6.7 \pm 0.8{:}3.5 \pm 0.2$ for complexes I/II/III/IV/V [32], and the levels of complex I subunits have also been found to be lower in cultured human cells [33]. In addition, transcriptional variation can occur. For example, complex I ND6 transcripts in 143B cells appear to be present at lower steady-state levels than do other mtDNA transcripts [34]. The ND6 subunit is the only protein in human mitochondria to be coded from the light strand of mtDNA, and this subunit is essential for complex I assembly [35]. Thus, the synthesis of ND6 may be the rate-limiting step for the synthesis of new complex I assemblies.

Although labeling and assembly rates might differ, analysis by BN–PAGE is suitable to detect the presence of assembly intermediates. The pattern of assembly has been well characterized for complex IV, and our results are consistent with those of others [13]. A number of different complex I assembly intermediates have also been identified from a variety of studies. ND1 has been detected in different intermediate or stalled complexes. Studying complex I in patient cells containing mtDNA and nuclear mutations, Antonicka and coworkers [12] found ND1-containing complexes at approximately 310, 380, 480, and 650 kDa. In contrast, Ugalde and coworkers [11] used Western blot analysis to study the reassembly of subunits after doxycycline-mediated depletion of complex I. In this case, they found ND1 and ND6 together in intermediate complexes of approximately 400, 700, and 950 kDa. Our results with detecting only mtDNA-encoded subunits labeled within a 2 h window also show ND1 in what appears to be two intermediates of approximately 350 and 400 kDa. ND4 also migrated in an intermediate complex similar in size to ND1, consistent with data from *N. crassa* where these two subunits are both components of the same membrane arm subcomplex [36]. The appearance of ND2 in a different subcomplex (~450 kDa) from that of ND1 and ND4 also concurs with the *N. crassa* model [36].

The chase experiments also identified a novel approximately 120 kDa species that contains cytochrome *b*. This species may be similar to one of the assembly intermediates that has been proposed in the yeast complex III assembly pathway [28,29]. It appears that in humans, cytochrome *b* assembles via this putative approximately 120 kDa intermediate into the dimeric enzyme ($CIII_2$) before forming supercomplexes with complexes I and IV (Fig. 3). This is further supported by our results in Fig. 2A using digitonin solubilization, where the complex III dimer ($CIII_2$) is observed before the $CI/CIII_2/CIV$ supercomplex forms. In contrast, complex I subunits appear to assemble at equal efficiency into either the complex I holoenzyme or the supercomplex. These results are consistent with the biogenesis of complex III being independent of complex I, whereas assembly of complex I and its supercomplex is dependent on complex III [18].

The radiolabeling of mtDNA-encoded translation products is also useful for the analysis of assembly defects in patient cell lines. In our hands, we were able to correlate these defects with previously identified respiratory chain enzymatic deficiencies. This potential diagnostic approach can be used in two ways. First, the assay can be performed with a single extended chase time point to identify possible assembly defects in the complex I, III, IV, or V holoenzymes in a single assay without the need to immunodecorate with a suite of antibodies. Second, detailed pulse/chase labeling with multiple time points can be performed to identify where defects occur in the assembly pathway. Either of these methodologies can be employed to examine cells from patients with more complex etiologies, thereby leading to the prioritization of candidate genes for

mutation analysis [37]. These approaches may also be extended to characterizing defects in respiratory complex assembly in other more common disorders where OXPHOS defects have been implicated such as diabetes, Parkinson's and Alzheimer's diseases, and apoptosis and aging [38].

In conclusion, we have combined mtDNA-encoded subunit labeling and BN–PAGE for the examination of respiratory complex assembly, and we propose that it is a useful technique both for the analysis of complex biogenesis and as a diagnostic tool for identifying assembly defects in mitochondrial disease patients.

Acknowledgments

We thank N. Hoogenraad for discussions, J. Hoogenraad for cell culture, I. Trounce for cell lines, and A. Lombes for the ND1 antibody. This work was supported by grants from the National Health and Medical Research Council (NHMRC, 280615 and 237137) and the Muscular Dystrophy Association. M.M. is supported by an NHMRC Peter Doherty Fellowship (380840), D.R.T. is supported by an NHMRC Senior Research Fellowship (216721), and M.L. is supported by an Australian Postgraduate Award.

References

[1] D.C. Wallace, Mitochondrial diseases in man and mouse, Science 283 (1999) 1482–1488.
[2] N.J. Hoogenraad, L.A. Ward, M.T. Ryan, Import and assembly of proteins into mitochondria of mammalian cells, Biochim. Biophys. Acta 1592 (2002) 97–105.
[3] A. Chomyn, P. Mariottini, M.W. Cleeter, C.I. Ragan, A. Matsuno-Yagi, Y. Hatefi, R.F. Doolittle, G. Attardi, Six unidentified reading frames of human mitochondrial DNA encode components of the respiratory-chain NADH dehydrogenase, Nature 314 (1985) 592–597.
[4] A. Chomyn, M.W. Cleeter, C.I. Ragan, M. Riley, R.F. Doolittle, G. Attardi, URF6, last unidentified reading frame of human mtDNA, codes for an NADH dehydrogenase subunit, Science 234 (1986) 614–618.
[5] J.A. Enriquez, A. Chomyn, G. Attardi, MtDNA mutation in MERRF syndrome causes defective aminoacylation of tRNA(Lys) and premature translation termination, Nat. Genet. 10 (1995) 47–55.
[6] M.P. King, Y. Koga, M. Davidson, E.A. Schon, Defects in mitochondrial protein synthesis and respiratory chain activity segregate with the tRNA(Leu(UUR)) mutation associated with mitochondrial myopathy, encephalopathy, lactic acidosis, and strokelike episodes, Mol. Cell Biol. 12 (1992) 480–490.
[7] G. Hofhaus, G. Attardi, Lack of assembly of mitochondrial DNA-encoded subunits of respiratory NADH dehydrogenase and loss of enzyme activity in a human cell mutant lacking the mitochondrial ND4 gene product, EMBO J. 12 (1993) 3043–3048.
[8] G. Hofhaus, G. Attardi, Efficient selection and characterization of mutants of a human cell line which are defective in mitochondrial DNA-encoded subunits of respiratory NADH dehydrogenase, Mol. Cell. Biol. 15 (1995) 964–974.
[9] H. Schagger, G. von Jagow, Blue Native electrophoresis for isolation of membrane protein complexes in enzymatically active form, Anal. Biochem. 199 (1991) 223–231.
[10] C. Ugalde, R.J. Janssen, L.P. van den Heuvel, J.A. Smeitink, L.G. Nijtmans, Differences in assembly or stability of complex I and other mitochondrial OXPHOS complexes in inherited complex I deficiency, Hum. Mol. Genet. 13 (2004) 659–667.
[11] C. Ugalde, R. Vogel, R. Huijbens, B. Van den Heuvel, J. Smeitink, L. Nijtmans, Human mitochondrial complex I assembles through the combination of evolutionary conserved modules: A framework to interpret complex I deficiencies, Hum. Mol. Genet. 13 (2004) 2461–2472.
[12] H. Antonicka, I. Ogilvie, T. Taivassalo, R.P. Anitori, R.G. Haller, J. Vissing, N.G. Kennaway, E.A. Shoubridge, Identification and characterization of a common set of complex I assembly intermediates in mitochondria from patients with complex I deficiency, J. Biol. Chem. 278 (2003) 43081–43088.
[13] L.G. Nijtmans, J.W. Taanman, A.O. Muijsers, D. Speijer, C. Van den Bogert, Assembly of cytochrome-*c* oxidase in cultured human cells, Eur. J. Biochem. 254 (1998) 389–394.
[14] H. Schagger, K. Pfeiffer, Supercomplexes in the respiratory chains of yeast and mammalian mitochondria, EMBO J. 19 (2000) 1777–1783.
[15] D.M. Kirby, R. Salemi, C. Sugiana, A. Ohtake, L. Parry, K.M. Bell, E.P. Kirk, A. Boneh, R.W. Taylor, H.H. Dahl, M.T. Ryan, D.R. Thorburn, NDUFS6 mutations are a novel cause of lethal neonatal mitochondrial complex I deficiency, J. Clin. Invest. 114 (2004) 837–845.
[16] H. Schagger, Respiratory chain supercomplexes, IUBMB Life 52 (2001) 119–128.
[17] R. Acin-Perez, M.P. Bayona-Bafaluy, P. Fernandez-Silva, R. Moreno-Loshuertos, A. Perez-Martos, C. Bruno, C.T. Moraes, J.A. Enriquez, Respiratory complex III is required to maintain complex I in mammalian mitochondria, Mol. Cell 13 (2004) 805–815.
[18] H. Schagger, R. de Coo, M.F. Bauer, S. Hofmann, C. Godinot, U. Brandt, Significance of respirasomes for the assembly/stability of human respiratory chain complex I, J. Biol. Chem. 279 (2004) 36349–36353.
[19] M. McKenzie, M. Lazarou, D.R. Thorburn, M.T. Ryan, Mitochondrial respiratory chain supercomplexes are destabilized in Barth syndrome patients, J. Mol. Biol. 361 (2006) 462–469.
[20] D.M. Kirby, M. Crawford, M.A. Cleary, H.H. Dahl, X. Dennett, D.R. Thorburn, Respiratory chain complex I deficiency: An underdiagnosed energy generation disorder, Neurology 52 (1999) 1255–1264.
[21] A. Chomyn, In vivo labeling and analysis of human mitochondrial translation products, Methods Enzymol. 264 (1996) 197–211.
[22] H. Schagger, G. von Jagow, Tricine–sodium dodecyl sulfate–polyacrylamide gel electrophoresis for the separation of proteins in the range from 1 to 100 kDa, Anal. Biochem. 166 (1987) 368–379.
[23] A.J. Johnston, J. Hoogenraad, D.A. Dougan, K.N. Truscott, M. Yano, M. Mori, N.J. Hoogenraad, M.T. Ryan, Insertion and assembly of human tom7 into the preprotein translocase complex of the outer mitochondrial membrane, J. Biol. Chem. 277 (2002) 42197–42204.
[24] P. Costantino, G. Attardi, Metabolic properties of the products of mitochondrial protein synthesis in HeLa cells, J. Biol. Chem. 252 (1977) 1702–1711.
[25] N. Yadava, P. Potluri, E.N. Smith, A. Bisevac, I.E. Scheffler, Species-specific and mutant MWFE proteins: Their effect on the assembly of a functional mammalian mitochondrial complex I, J. Biol. Chem. 277 (2002) 21221–21230.
[26] I. Ogilvie, N.G. Kennaway, E.A. Shoubridge, A molecular chaperone for mitochondrial complex I assembly is mutated in a progressive encephalopathy, J. Clin. Invest. 115 (2005) 2784–2792.
[27] V. Tiranti, C. Galimberti, L. Nijtmans, S. Bovolenta, M.P. Perini, M. Zeviani, Characterization of SURF-1 expression and Surf-1p function in normal and disease conditions, Hum. Mol. Genet. 8 (1999) 2533–2540.
[28] Z. Kronekova, G. Rodel, Organization of assembly factors Cbp3p and Cbp4p and their effect on bc_1 complex assembly in *Saccharomyces cerevisiae*, Curr. Genet. 47 (2005) 203–212.
[29] V. Zara, I. Palmisano, L. Conte, B.L. Trumpower, Further insights into the assembly of the yeast cytochrome bc_1 complex based on

analysis of single and double deletion mutants lacking supernumerary subunits and cytochrome *b*, Eur. J. Biochem. 271 (2004) 1209–1218.
[30] M.D. Crivellone, M.A. Wu, A. Tzagoloff, Assembly of the mitochondrial membrane system: Analysis of structural mutants of the yeast coenzyme QH2–cytochrome *c* reductase complex, J. Biol. Chem. 263 (1988) 14323–14333.
[31] E.A. Shoubridge, Cytochrome *c* oxidase deficiency, Am. J. Med. Genet. 106 (2001) 46–52.
[32] H. Schagger, K. Pfeiffer, The ratio of oxidative phosphorylation complexes I–V in bovine heart mitochondria and the composition of respiratory chain supercomplexes, J. Biol. Chem. 276 (2001) 37861–37867.
[33] L.G. Nijtmans, P. Klement, J. Houstek, C. van den Bogert, Assembly of mitochondrial ATP synthase in cultured human cells: Implications for mitochondrial diseases, Biochim. Biophys. Acta 1272 (1995) 190–198.
[34] H. Duborjal, R. Beugnot, B.M. De Camaret, J.P. Issartel, Large functional range of steady-state levels of nuclear and mitochondrial transcripts coding for the subunits of the human mitochondrial OXPHOS system, Genome Res. 12 (2002) 1901–1909.
[35] Y. Bai, G. Attardi, The mtDNA-encoded ND6 subunit of mitochondrial NADH dehydrogenase is essential for the assembly of the membrane arm and the respiratory function of the enzyme, EMBO J. 17 (1998) 4848–4858.
[36] R. Kuffner, A. Rohr, A. Schmiede, C. Krull, U. Schulte, Involvement of two novel chaperones in the assembly of mitochondrial NADH:ubiquinone oxidoreductase (complex I), J. Mol. Biol. 283 (1998) 409–417.
[37] D.R. Thorburn, C. Sugiana, R. Salemi, D.M. Kirby, L. Worgan, A. Ohtake, M.T. Ryan, Biochemical and molecular diagnosis of mitochondrial respiratory chain disorders, Biochim. Biophys. Acta 1659 (2004) 121–128.
[38] D.C. Wallace, A mitochondrial paradigm of metabolic and degenerative diseases, aging, and cancer: A dawn for evolutionary medicine, Annu. Rev. Genet. 39 (2005) 359–407.